Sulfur–Functionalized Fullerene Nanoparticle as an Inhibitor and Eliminator Agent on Pseudomonas aeruginosa Biofilm and Expression of toxA Gene

Article *in* Microbial Drug Resistance · November 2018

DOI: 10.1089/mdr.2018.0008

CITATION
1

READS
36

4 authors, including:

Raheleh Halabian
Baqiyatallah University of Medical Sciences
96 PUBLICATIONS **857** CITATIONS

SEE PROFILE

Abbas Ali Imani Fooladi
260 PUBLICATIONS **2,253** CITATIONS

SEE PROFILE

MICROBIAL DRUG RESISTANCE
Volume 00, Number 00, 2018

DOI: 10.1089/mdr.2018.0008

Sulfur-Functionalized Fullerene Nanoparticle as an Inhibitor and Eliminator Agent on *Pseudomonas aeruginosa* Biofilm and Expression of *toxA* Gene

Esmaeil Darabpour,[1] Mohammad Mahdi Doroodmand,[2] Raheleh Halabian,[1] and Abbas Ali Imani Fooladi[1]

Over the last decade, nanotechnology-based therapeutic platforms have been directed toward developing nanoparticles with unique properties to combat biofilms. In this study, we evaluated the antibiofilm activity of the sulfur-functionalized fullerene nanoparticles (SFF Nps) against *Pseudomonas aeruginosa* and also analyzed the effect of this nanoparticle on the expression *of exotoxin A* (*toxA*) gene. The functionalized fullerenes were prepared by chemical vapor deposition method. We assessed the potential of SFF Nps to inhibit biofilm formation and eradicate preformed biofilms. Also, the effect of this nanoparticle on the expression of *toxA* gene was investigated by real-time PCR. The minimum biofilm inhibitory concentration of SFF Nps was 1 mg/mL. The minimum biofilm-eradication concentration of SFF Nps on the young (24- and 48-hr old) and older (72- and 96-hr old) biofilms was 2 and 4 mg/mL, respectively. Field emission electron scanning microscopy images confirmed the potent ability of SFF Nps to eradicate biofilm of *P. aeruginosa*. The expression of *toxA* was downregulated in the presence of SFF Nps. In conclusion, considering the ability of SFF Nps to kill *P. aeruginosa* biofilm and downregulate the expression of *exotoxin A*, this nanoparticle can be used for treatment of both chronic and acute *P. aeruginosa* infections.

Keywords: functionalized fullerene nanoparticle, biofilm, real-time PCR, wound infection

Introduction

Pseudomonas aeruginosa is an opportunistic human pathogen that may cause infections with substantial morbidity and mortality, particularly in patients with cystic fibrosis, burns, and immunosuppression.[1] This bacterium is considered one of a group of six highly antibiotic-resistant pathogens responsible for nosocomial infections (the ESKAPE pathogens, *i.e.*, *Enterococcus faecium*, *Staphylococcus aureus*, *Klebsiella pneumoniae*, *Acinetobacter baumannii*, *P. aeruginosa*, and *Enterobacter* species).[2,3]

P. aeruginosa produces a variety of virulence factors that allow it to cause acute and chronic infections.[4] The pathogenesis of acute *P. aeruginosa* infections has implicated virulence factors such as *exotoxin A* (encoded by the *toxA* gene), as the most toxic substance produced by *P. aeruginosa,* which inhibits protein synthesis and induces apoptosis.[5] *Exotoxin A* is one of the main virulence factors secreted by *P. aeruginosa*, which plays an important role in impeding wound healing.[6] The pathogenesis of chronic *P. aeruginosa* infections is mainly due to the capacity of this bacterium to form biofilms, which are structured communities of sessile bacterial cells that are encased in a self-produced matrix of extracellular polymeric substances (EPS) comprising polysaccharides, proteins, and extracellular DNA, during the infection process.[7–9] Quorum sensing, a cell-to-cell communication mechanism, plays a major role in the biofilm development of many bacterial pathogens such as *P. aeruginosa*; also, this mechanism plays a critical role in the regulation of *toxA* (*exotoxin A*).[10,11]

Bacteria growing in a biofilm may evade host immune defenses and become tolerant to concentrations of antimicrobials that eliminate free-swimming (planktonic) single cells, so there is an urgent need to develop effective alternative therapeutic approaches that target biofilm-related infections.[12]

Nanotechnology can be considered a new promising tool to provide solutions for this problem. Some of the previously reported studies demonstrated that silver nanoparticles can both prevent biofilm formation and disrupt existing biofilm of *P. aeruginosa*.[13,14] However, there are rare reports about the potential application of other nanoparticles against biofilms. Fullerenes (C_{60}, C_{70}, etc.) are carbon nanomaterials that, due to its unique carbon cage structure coupled with immense scope for derivatization, have attracted

[1]Applied Microbiology Research Center, Systems Biology and Poisonings Institute, Baqiyatallah University of Medical Sciences, Tehran, Iran.
[2]Department of Chemistry, College of Sciences, Shiraz University, Shiraz, Iran.

significant attention in various biomedical fields, including drug/gene delivery and antiviral, antibacterial, and anticancer agents.[15–18] Chemical functionalization of fullerenes can give derivatives with specific chemical and biological properties, compared to pristine fullerenes. According to previous studies, sulfur-containing organic and inorganic compounds appear to be a new class of molecules capable of killing bacteria and inhibiting quorum sensing.[19,20] Hereby, we aimed to investigate the antibiofilm activity of sulfur-functionalized fullerene (C_{60}) nanoparticle derivative against *P. aeruginosa* and analyze the effect of this nanoparticle on the expression of *toxA* gene.

Materials and Methods

Synthesis and characterization of sulfur-functionalized fullerene nanoparticles

All the chemical reagents were from their analytical grades. To fabricate the sulfur-functionalized fullerene nanoparticles (SFF Nps), briefly fullerene nanoparticles with ~99% purity were synthesized by chemical vapor deposition (CVD) method.[21,22] For this purpose, acetylene (Pasbaloon, Shiraz, Iran) was selected as the source of carbon in an inert atmosphere of Ar/He (1:1, V/V; Linde, Germany) at 1,200°C inside quartz tubing situated in a tubing furnace. To synthesize the fullerene, Fe nanoparticles acted as both the catalyst and the solid support for the deposition of the carbon vapors. To synthesize the Fe nanoparticles, solution of ferrocene (Merck, Germany) in toluene (Fluka analytical grade, Germany) was prepared. To reach this aim, ~15 weight percentage solution was prepared using ferrocene in toluene. Also, around 1% (V/V) thiophene (Fluka), as a sulfur source, was added to the solution for lengthening the CVD-synthesized fullerene bucky balls.[23]

Size and morphology of the formed nanoparticles were investigated by a scanning electron microscope (SEM). The CVD-synthesized nanoparticles were characterized by X-ray diffraction (XRD), Raman spectroscopy, and SEM. The stock solution (8 mg/mL) of SFF Nps were prepared in DMSO (4%) and stored at room temperature.

Bacterial strain and culture conditions

The microorganism used in this study was a multidrug-resistant (MDR) strain of *P. aeruginosa*. This strain was a clinical isolate recovered from a chronic wound and showed resistance to the following antibiotics: norfloxacin (10 μg), ciprofloxacin (5 μg), imipenem (10 μg), ceftazidime (30 μg), and gentamicin (10 μg). All of the synthetic antibiotic discs were produced by Padtan Teb Company (Iran).

The strain was maintained by regular subculture on nutrient agar (NA; Merck, Germany) plates. To prepare inoculum, the test strain was grown aerobically overnight at 37°C on NA plates and then a suspension of strain was prepared in sterile phosphate-buffered saline (PBS, pH 7.4) to reach the turbidity of 0.5 McFarland (a concentration of 1.5×10^8 CFU/mL).[24,25] Tryptic Soy Broth (TSB; Merck) was used as the liquid medium for biofilm culture.

Biofilm formation assay

Biofilm was formed by growing the bacterium on polystyrene 96-well microtiter plates. Crystal violet assay was used to quantify the formed biofilm. Overnight culture of *P. aeruginosa* strain was diluted at 1:50 in the TSB supplemented with 0.2% glucose. Aliquots (200 μL) of this cell suspension were added to 6 wells of a 96-well flat-bottomed sterile polystyrene microplate and incubated for 24 hr at 37°C. After incubation, the medium was removed, and the wells were washed twice with PBS (pH 7.4) to remove planktonic cells. The attached bacteria remaining were fixed with 95% ethanol for 10 min and then were stained with 0.4% crystal violet for 15 min. Following the staining step, the wells were rinsed several times with PBS and air dried. For the quantitative estimation of biofilm density, crystal violet was solubilized with 10% glacial acetic acid and absorbance of the solubilized dye was read at 492 nm (optical density [OD] 492) using a microplate reader (Hiperion MPR4+, Germany).[26–28]

Considering a low cutoff (ODc) defined as $3\times$SD above the mean OD of control wells (uninoculated wells containing TSB), strain was classified into the following categories: no biofilm producer (OD ≤ ODc), weak biofilm producer (ODc < OD ≤$2\times$ODc), moderate biofilm producer ($2\times$ODc < OD ≤$4\times$ODc), and strong biofilm producer ($4\times$ODc < OD).[25]

Biofilm inhibition assay

The bacterial suspension with a turbidity equivalent to a McFarland standard of 0.5 (corresponding to 1.5×10^8 CFU/mL) was diluted at 1:50 in TSB supplemented with 0.2% glucose. Aliquots (100 μL) of the diluted cell suspension were inoculated into 96-well flat-bottomed sterile polystyrene microplates. The SFF Nps were diluted (in TSB supplied with 4% DMSO) twofold from a stock concentration of 4 mg/mL. One hundred microliters of the diluted SFF Nps was then added to the suspension and incubated for 24 hr at 37°C. Appropriate controls were also included. Inhibition of biofilm growth was quantified using the crystal violet assay as described above, and the percentage of biofilm inhibition was calculated as $[1 - (OD_{492}$ of cells treated with test agent/OD_{492} of untreated control)]$\times100$. The minimum biofilm inhibitory concentration (MBIC) was defined as the lowest concentration that inhibited at least 90% biofilm formation.[29,30] Experiments were performed in triplicate.

Biofilm eradication assay

Minimum biofilm eradication concentration (MBEC) of SFF Nps on cell viability in 24-hr and 4-day-old biofilms of *P. aeruginosa* was determined by 2,3,5-triphenyltetrazolium chloride (TTC) reduction assay.[31]

Biofilms were grown in 96-well microtiter plates as described above using the culture medium TSB. Fresh TSB medium was replenished daily to provide a constant supply of nutrients and to remove planktonic (nonadherent) cells.[25,32] On the first and fourth day, the growth medium was carefully aspirated and the wells were washed twice with fresh PBS (pH 7.4). Twofold serial dilutions (ranging between 4 and 1 mg) of SFF Nps were prepared in TSB. Then, 200 μL of each concentration was added, and the plate was incubated for 25 min (among different incubation times, 25 min as the minimum time required to eradicate the biofilm was chosen for further studies [data not shown]) at 37°C. At the end of incubation, TTC was added at a final

concentration of 0.005 mg/mL, and the plate was incubated for 24 hr at 37°C. Surviving bacteria metabolize the TTC and produce red formazan. After the incubation period, absorbance was read at 492 nm using a microplate reader (Hiperion MPR4+). The percentage of biofilm viability was calculated as $[1 - (OD_{492}$ of cells treated with test agent/ OD_{492} of untreated control)] $\times 100$. The minimum biofilm eradication concentration (MBEC) was defined as the lowest concentration of SFF Nps that decreased biofilm viability by at least 90%.[33]

Ultrastructural study on the antibiofilm activity of SFF Nps by field emission electron scanning microscopy

The effect of the SFF Nps on preformed *P. aeruginosa* biofilm was further evaluated by field emission electron scanning microscopy (FESEM). At first, biofilms were grown on the surface of sterile glass pieces (1×1 cm) placed in 48-well microtiter plate. After 24 hr, the glass pieces were rinsed twice with PBS to remove nonadherent cells. Preformed biofilms were treated with one-half MBEC and MBEC values of SFF Nps for 25 min at 37°C. Then, the glass pieces containing the treated biofilm and control biofilm (in the absence of nanoparticles) were washed with sterile PBS and fixed with a glutaraldehyde solution (2.5%, V/V) for 1 hr at 4°C.

Following fixation, the samples were washed with water and dehydrated in a graded series of ethanol solutions (30%, 50%, 70%, 80%, 90%, and 100%; 15 min each step). Before visualization, samples were freeze dried and then sputter coated with gold. The surface morphology of biofilms was visualized using a field emission scanning electron microscope (HT7700; Hitachi, Tokyo, Japan) by selecting a voltage of 15 kV.[34]

Isolation of bacterial RNA and reverse transcription

The effect of SFF Nps at sub-MBIC on the expression of *toxA* gene was assessed by real-time PCR. For this purpose, the strain was grown (under the same experimental conditions as used for the biofilm formation assay) in the absence or presence of SFF Nps at its one-half MBIC for 30 min and 24 hr at 37°C and then, bacterial cells were collected for RNA extraction.

The bacterial RNA was isolated from 1×10^6 bacterial cells. In brief, the cell culture was collected and centrifuged to recover the bacterial cells, which were then resuspended in 2 mL of cold PBS. RNA extraction was carried out on the thawed samples according to the manufacturer's protocol. The precipitated RNA was resuspended in 30 μL DEPC water and 1 μg of RNA was reverse transcribed with 200U SuperScript™ III Reverse Transcriptase (Invitrogen) for 60 min at 50°C using Oligo-dT in a 20 μL volume.

Real-time quantitative

PCR was performed using the Rotor gene Q (Qiagen) in 0.2 mL microtube using a final volume of 25 μL for *toxA* gene primers (F: 5′-TGCTGCACTACTCCATGGTC-3′ and R: 5′-ATCGGTACCAGCCAGTTCAG-3′). Amplifications were performed starting with a 2-min activation step for Amperase® UNG at 50°C, 10-min template denaturation step at 95°C, followed by 40 cycles of 95°C for 15 sec and 60°C for 1 min.

Quantitative real-time PCR efficiency and intra-assay and interassay variability

Quantitative real-time PCR was used to measure the RNA transcription level of various candidate *toxA* genes. To compare different RNA transcription levels, the Ct values were compared directly. The Ct is defined as the number of cycles needed for the fluorescence to reach a specific threshold level of detection and is inversely correlated with the amount of template nucleic acid present in the reaction.[35]

Statistical analysis

Comparisons between means of groups were analyzed using the one-way ANOVA and *post hoc* Tukey tests. $p < 0.05$ was considered statistically significant.

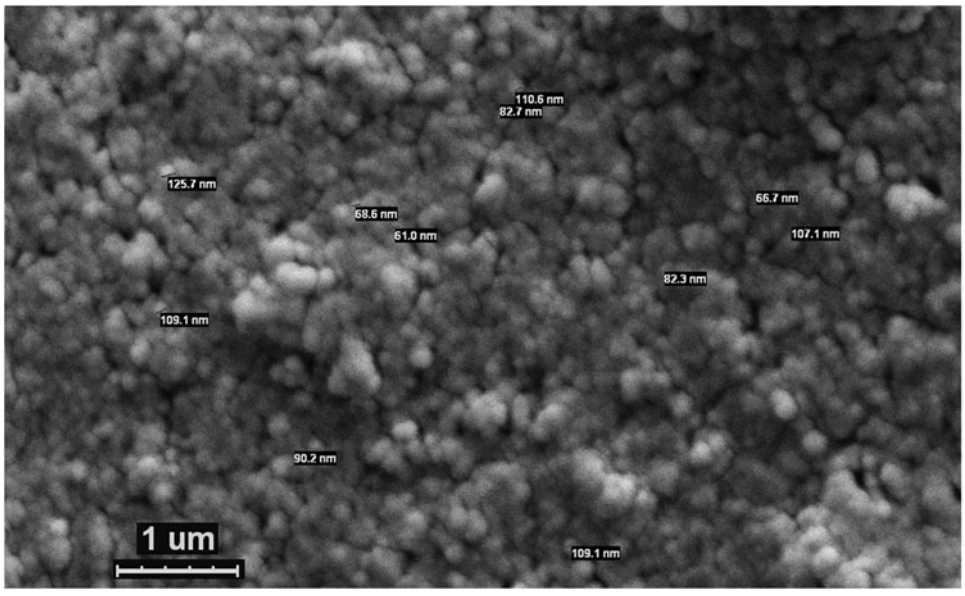

FIG. 1. SEM image of SFF Nps. The image represents the spherical shape of nanoparticles. SEM, scanning electron microscope; SFF Nps, sulfur-functionalized fullerene nanoparticles.

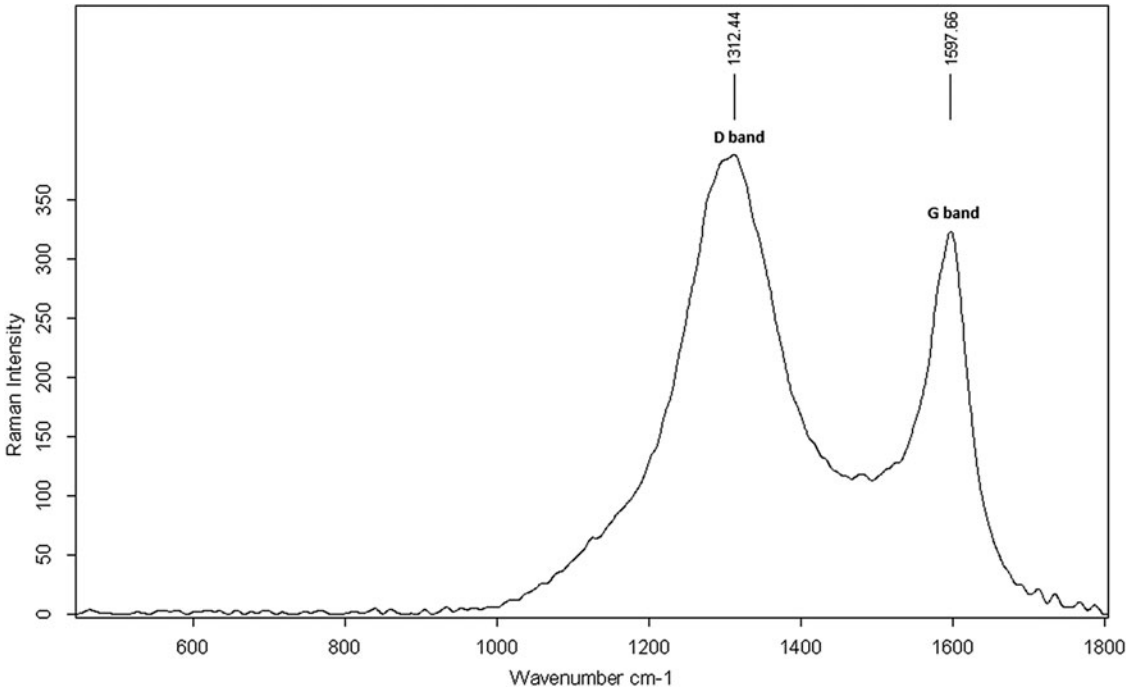

FIG. 2. Raman spectrum of SFF Nps.

Results

Characterization of SFF Nps

The SEM image of the prepared nanoparticles is shown in Fig. 1. As seen in the SEM image, SFF Nps are spherical in shape and a large percentage of them are available in sizes ranging from 60 to 110 nm in diameter.

Structural analyses of the SFF Nps were carried out by Raman spectroscopy and XRD. The D- and G-bands are clearly shown according to the Raman spectrum

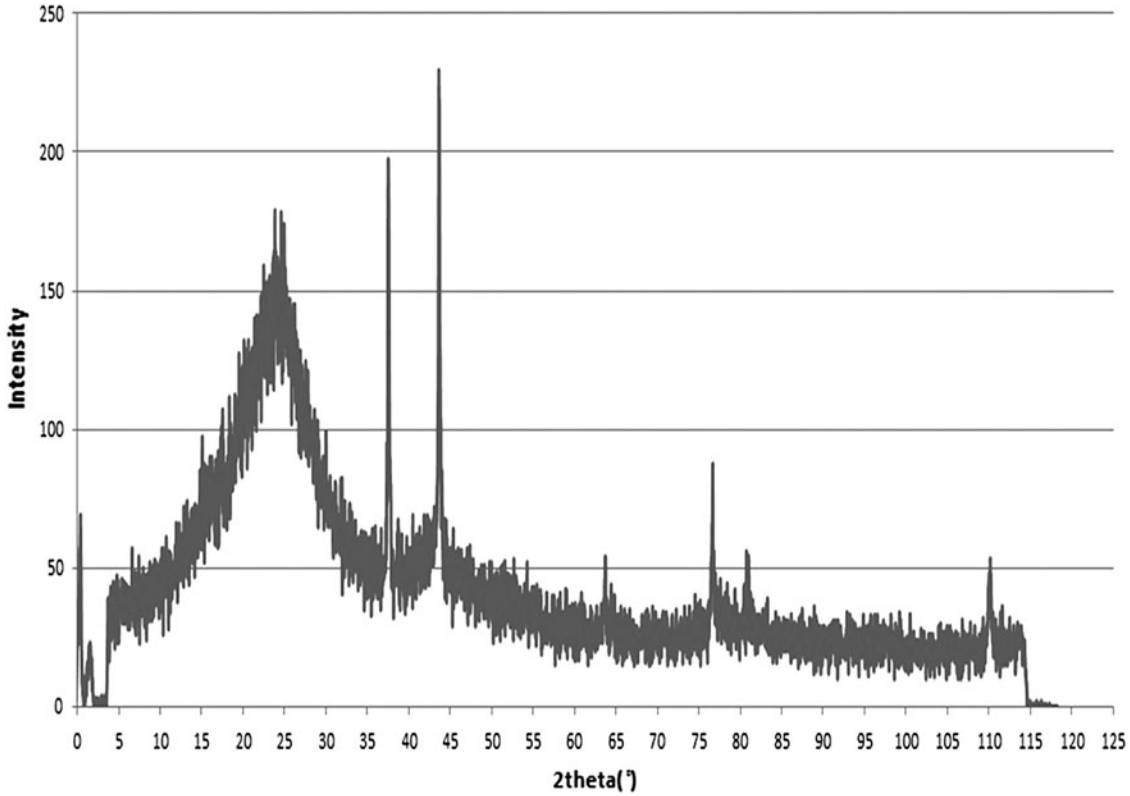

FIG. 3. XRD pattern of SFF Nps shows the characteristic peaks of sulfur and fullerene. XRD, X-ray diffraction.

(Fig. 2). According to the Raman spectrum, the defect of the synthesized SFF Nps was estimated to around 0.83. In addition, the XRD pattern of the CVD-synthesized SFF Nps shows the characteristic peaks of sulfur and fullerene (Fig. 3), which is in good agreement with the database of the sulfur- and carbon-based materials.

Effects of SFF Nps on biofilm formation by MDR P. aeruginosa *cells*

The microorganism used in this study was a strong biofilm producer. The amount of biofilm produced by MDR *P. aeruginosa* after 24 hr of growth in the presence of SFF Nps was determined by crystal violet staining of the adhered cells.

The results, which are presented in Fig. 4, showed that SFF Nps were effective in preventing biofilm formation by *P. aeruginosa*. SFF Nps significantly reduced biofilm formation by 92.2% at a concentration of 1 mg/mL, considered MBIC (Fig. 4) ($p < 0.5$). However, SFF Nps at the lowest tested concentration (0.125 mg/mL) did not significantly inhibit biofilm formation.

Biofilm formation was reduced gradually with increasing SFF Nps concentration, demonstrating that SFF Nps inhibited biofilm formation in a concentration-dependent manner. In addition, it was observed that 4% DMSO did not affect biofilm formation.

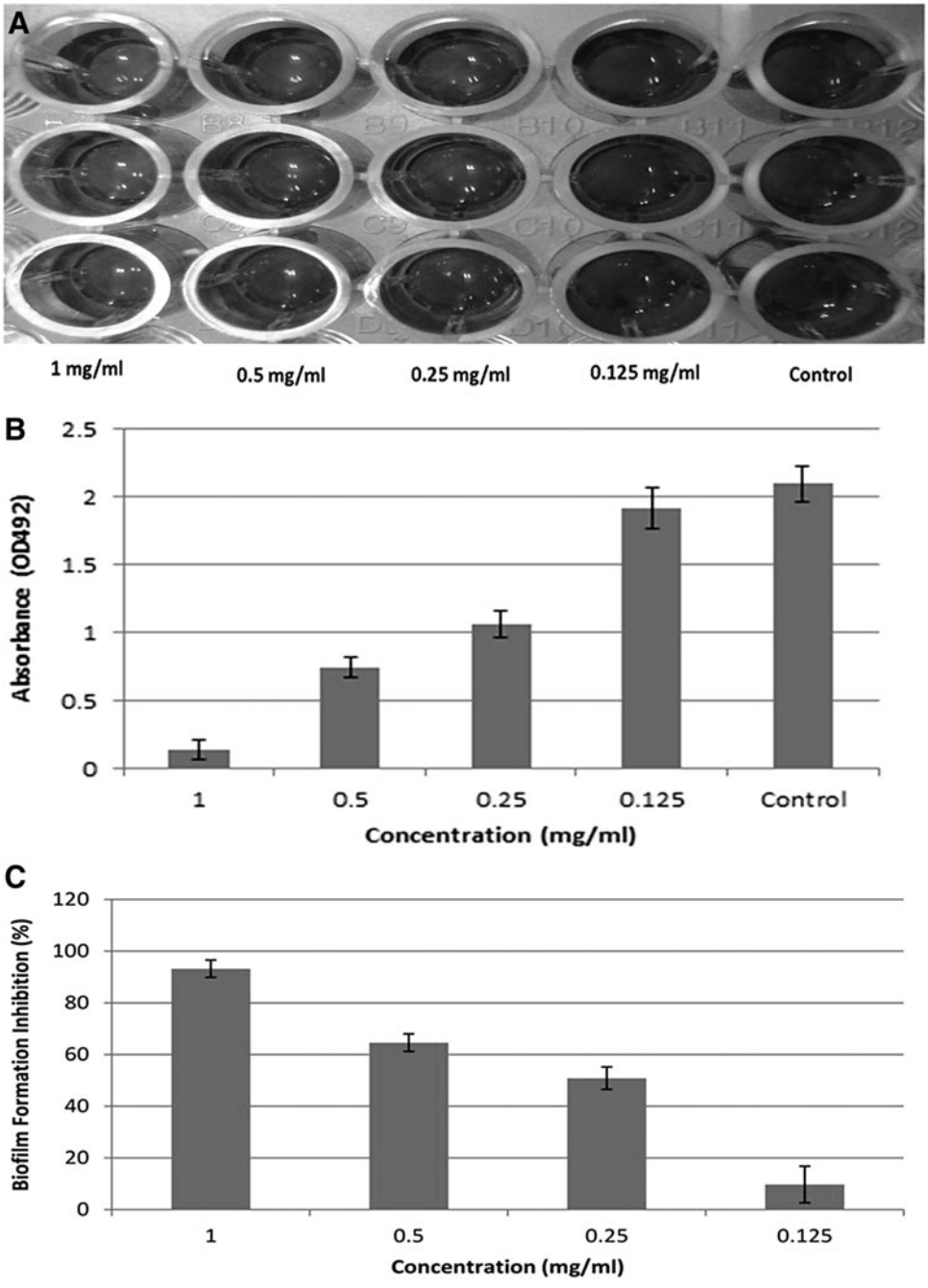

FIG. 4. Effect of different concentrations of SFF Nps on biofilm formation of *Pseudomonas aeruginosa* (24-hr-old biofilm). **(A)** Photograph showing biofilms grown with and without SFF Nps after crystal violet staining. **(B)** Quantification of crystal violet dye attached to the cells forming biofilms. **(C)** Percentage inhibition of *P. aeruginosa* biofilm grown in the presence of different concentrations of SFF Nps. ($p < 0.05$ was considered statistically significant).

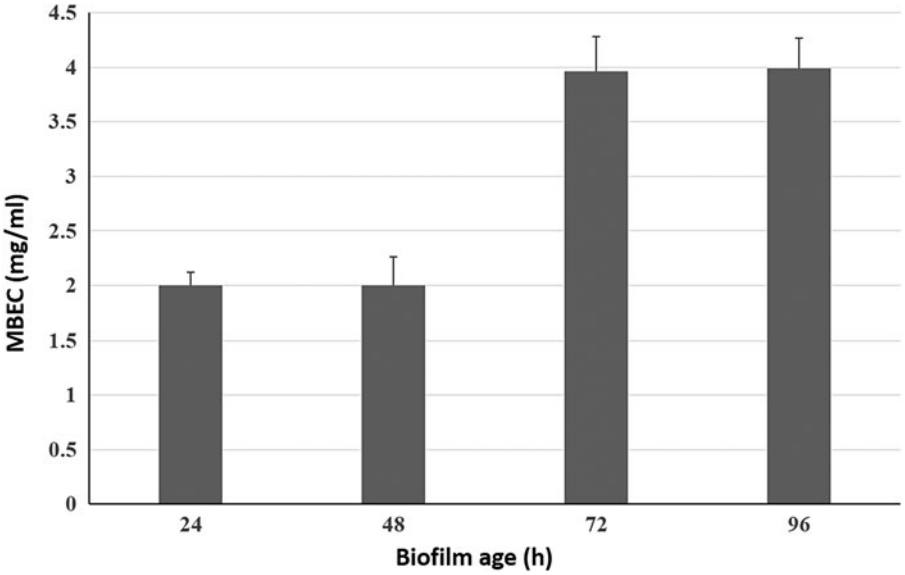

FIG. 5. Comparative susceptibility of *P. aeruginosa* biofilms of different ages to SFF Nps. MBEC, minimum biofilm eradication concentration.

Effect of SFF Nps on viability of P. aeruginosa *cells in biofilm*

We also studied the ability of SFF Nps to eliminate cells in established biofilms (1- to 4-day old). TTC assay was used to measure cell viability in biofilms with and without treatment. The results showed that SFF Nps had significant antibiofilm activity against *P. aeruginosa* even after aging (Fig. 5).

The MBEC of SFF Nps against 1- and 2-day-old *P. aeruginosa* biofilm was 2 mg/mL, while this value against older biofilms (3- and 4-day old) was 4 mg/mL (Fig. 5).

FESEM analysis of P. aeruginosa *biofilm structure after treatment with SFF Nps*

We used FESEM to directly visualize the effects of SFF Nps on *P. aeruginosa* biofilm structure and on the morphology of the bacterial cells within the biofilms. The control biofilm appeared as an intact structure consisting of numerous cells connected by a substantial amount of extracellular matrix (Fig. 6A). After treatment with SFF Nps at 1 mg/mL (one-half the MBEC), it was observed that the integrity of the biofilm structure was disrupted and bacterial

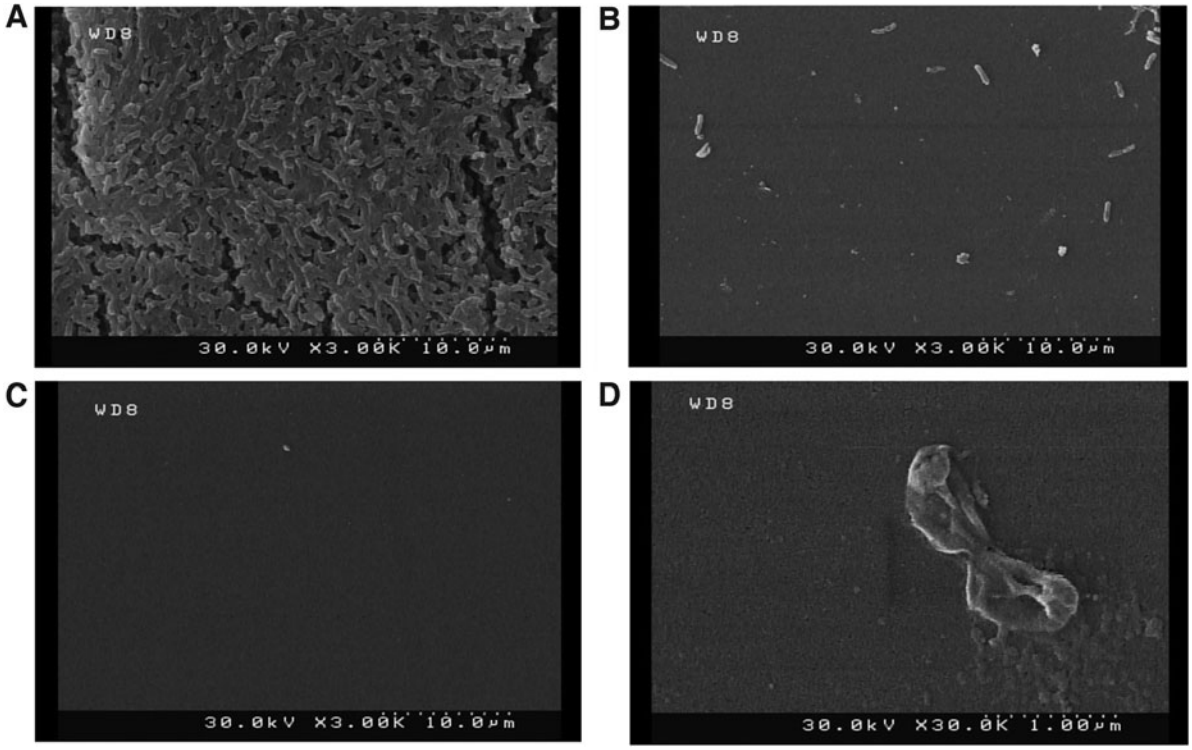

FIG. 6. SEM images of *P. aeruginosa* biofilm. **(A)** SEM micrograph of a preformed biofilm without treatment, **(B)** preformed biofilm after treatment with SFF Nps at 1 mg/mL (one-half the MBEC), **(C)** preformed biofilm after treatment with SFF Nps at 2 mg/mL (MBEC), and **(D)** the lysis of *P. aeruginosa* cell after treatment of the biofilm with SFF Nps.

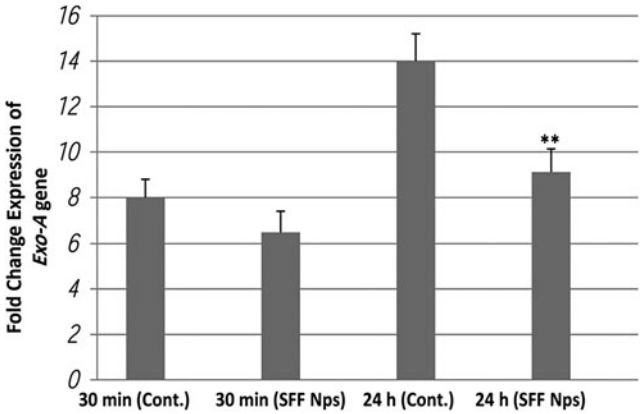

FIG. 7. Effect of SFF Nps at sub-MBIC (one-half MBIC) on the expression level of *toxA* gene. Cont., Control. $^{**}p < 0.05$. MBIC, minimum biofilm inhibitory concentration.

cell densities within the biofilm also decreased significantly (Fig. 6B). Biofilm of *P. aeruginosa* was completely eradicated by exposure to 2 mg/mL (MBEC) (Fig. 6C). As shown in Fig. 6D, the treated biofilm presented noticeable changes in cell morphology.

Inhibitory effect of SFF Nps on the expression of toxA

The effect of SFF Nps on the expression of *toxA* as a quorum sensing-regulated gene was measured by quantitative real-time PCR. Our data showed that the gene-level expression of *toxA* after 24-hr treatment with SFF Nps at one-half MBIC was significantly decreased compared to the untreated control group. However, after a 25-min treatment with SFF Nps, there was no significant difference between treated and untreated groups (Fig. 7).

Discussion

In recent years, nanoparticle-targeted antibiofilm therapy has gained significant attention due to their unique chemical and physical features. It has been reported that engineered nanoparticles can be considered potentially powerful vehicles to infiltrate into the EPS matrix, which acts as a barrier for many antibiotics.[36]

Fullerene is a novel nanomaterial with promising applications in the field of biomedicine. This study was aimed to develop SFF Nps to combat *P. aeruginosa* biofilm. Preventing biofilm formation by pathogenic bacteria is critical in the fight against healthcare-associated infections.[37] In this study, the impact of SFF Nps on biofilm formation by *P. aeruginosa* was determined performing the MBIC assay.

The results indicated that SFF Nps effectively prevented the initiation of biofilm formation even at ¼ of the MBIC value (by 51% biofilm inhibition), suggesting a strong inhibition of the bacterial adhesion (Fig. 4).

The exact mechanism of antimicrobial action of fullerene is not known; however, three possible mechanisms have been reported: (i) effect on respiratory chain, (ii) disruption of the cell membrane structure, and (iii) interaction with membrane lipids and intercalation into them.[38] It seems that the mechanism of antibiofilm activity of SFF Nps is associated with one or more than one of the above mechanisms. However, further studies should be performed to identify the exact mechanism of action of this nanoparticle against biofilm.

Biofilm eradication is a major challenge today to overcome chronic infections. In this study, the impact that SFF Nps had on preformed biofilms was also determined by performing the MBEC assay (Fig. 5). The results show that SFF Nps were effective against 24-hr-old biofilm of *P. aeruginosa*; >90% of the biofilm was eradicated at concentrations of 2 mg/mL (MBEC value).

The MBEC (2 mg/mL) was found to be twofold higher than MBIC (1 mg/mL). In general, MBEC is higher than MBIC, which might be due to the protective role of the extracellular matrix material of biofilms.[39]

The results also showed that the MBEC value of SFF Nps against 1- and 4-day-old biofilms was 2 and 4 mg/mL, respectively, indicating that bacteria in the older biofilms are more robust and protected.[40,41] In fact, due to increased production of EPS in older biofilm compared with younger biofilm, bacteria in older biofilm are more heavily encased in extracellular matrix than bacteria in young biofilm, so mature biofilm are less susceptible to antimicrobials than immature biofilm.[25] Meanwhile, a low ratio of MBEC value of 4- to 1-day-old biofilm demonstrated that SFF Nps are able to significantly eradicate *P. aeruginosa* in the biofilm form even after aging. Consequently, this nanoparticle can be effective against mature biofilms in chronic wounds.

FESEM analysis confirmed the findings obtained during MBEC assay. As evident from the FESEM images shown in Fig. 6, the initial dense layer of *P. aeruginosa* biofilm was substantially reduced following the treatment with SFF Nps, suggesting the good action of this nanoparticle against preformed biofilms.

Real-time PCR analysis showed that *toxA* was downregulated after adding SFF Nps at sub-MBIC in the biofilm formation. It is well known that the production of both biofilm and *exotoxin A* is regulated by quorum-sensing signals.[11] Therefore, we speculated that SFF Nps might attenuate *P. aeruginosa* biofilm formation by disturbing its quorum-sensing system. However, further study is necessary to determine the molecular mechanism by which SFF Nps inhibit biofilm formation by *P. aeruginosa.*

Conclusion

In this study, we developed a novel fullerene derivative (SFF Np derivative) and then, its antibiofilm efficacy was assessed against *P. aeruginosa.* Furthermore, we analyzed the effect of this nanoparticle on the expression *of exotoxin A* (*toxA*) gene.

In summary, this study demonstrated that SFF Nps possessed great efficacy to inhibit *P. aeruginosa* biofilm formation and are able to quickly and efficiently disrupt the multilayered, three-dimensional biofilm architecture even after aging, suggesting its potential use in chronic wound healing. Also, considering the ability of SFF Nps to downregulate the expression of *exotoxin A*, this nanoparticle can be used for treatment of acute *P. aeruginosa* infections such as acute wound infection.

Acknowledgments

The authors wish to acknowledge the support of this work by the Tehran Council, Shiraz Research Council and

Applied Microbiology Research Center (AMRC) of Baqiyatallah University of Medical Sciences (BUMS).

Disclosure Statement

No competing financial interests exist.

References

1. Gellatly, S.L., and R.E. Hancock. 2013. *Pseudomonas aeruginosa*: new insights into pathogenesis and host defenses. Pathog. Dis. 67:159–173.
2. Pukatzki, S., R.H. Kessin, and J.J. Mekalanos. 2002. The human pathogen *Pseudomonas aeruginosa* utilizes conserved virulence pathways to infect the social *amoeba Dictyostelium discoideum.* Proc. Natl. Acad. Sci. U.S.A. 99:3159–3164.
3. Gallagher, L.A., E. Ramage, E.J. Weiss, M. Radey, H.S. Hayden, K.G. Held, H.K. Huse, D.V. Zurawski, M.J. Brittnacher, and C. Manoil. 2015. Resources for genetic and genomic analysis of emerging pathogen *Acinetobacter baumannii.* J. Bacteriol. 197:2027–2035.
4. Lee, J.H., Y.G. Kim, M.H. Cho, and J. Lee. 2014. ZnO nanoparticles inhibit *Pseudomonas aeruginosa* biofilm formation and virulence factor production. Microbiol. Res. 169:888–896.
5. Luo, J., B. Dong, K. Wang, S. Cai, T. Liu, X. Cheng, D. Lei, Y. Chen, Y. Li, J. Kong, and Y. Chen. 2017. Baicalin inhibits biofilm formation, attenuates the quorum sensing-controlled virulence and enhances *Pseudomonas aeruginosa* clearance in a mouse peritoneal implant infection model. PLoS One 12:e0176883.
6. Wang, G.Q., T.T. Li, Z.R. Li, L.C. Zhang, L.H. Zhang, L. Han, and P.F. Tang. 2016. Effect of negative pressure on proliferation, virulence factor secretion, biofilm formation, and virulence-regulated gene expression of *Pseudomonas aeruginosa* in vitro. Biomed. Res. Int. 2016:425–432.
7. Mishra, M., G. Parise, K.D. Jackson, D.J. Wozniak, and R. Deora. 2005. The BvgAS signal transduction system regulates biofilm development in *Bordetella.* J. Bacteriol. 187: 1474–1484.
8. Furiga, A., B. Lajoie, S.E.L. Hage, G. Baziard, and C. Roques. 2016. Impairment of *Pseudomonas aeruginosa* biofilm resistance to antibiotics by combining the drugs with a new quorum-sensing inhibitor. Antimicrob. Agents Chemother. 60:1676–1686.
9. Gloag, E.S., L. Turnbull, A. Huang, P. Vallotton, H. Wang, L.M. Nolan, L. Mililli, C. Hunt, J. Lu, S.R. Osvath, L.G. Monahan, R. Cavaliere, I.G. Charles, M.P. Wang, M.L. Gee, R. Prabhakar, and C.B. Whitchurch. 2013. Self-organization of bacterial biofilms is facilitated by extracellular DNA. Proc. Natl. Acad. Sci. U.S.A. 110:11541–11546.
10. De Kievit, T. 2009. Quorum sensing in *Pseudomonas aeruginosa* biofilms. Environ. Microbiol. 11:279–288.
11. Shirtliff, M.E., J.T. Mader, and A.K. Camper. 2002. Molecular interactions in biofilms. Chem. Biol. 9:859–871.
12. Chen, M., Q. Yu, and H. Sun. 2013. Novel strategies for the prevention and treatment of biofilm related infections. Int. J. Mol. Sci. 14:18488–18501.
13. Sadekuzzaman, M., S. Yang, M.F.R. Mizan, and S.D. Ha. 2015. Current and recent advanced strategies for combating biofilms. Compr. Rev. Food Sci. Food Saf. 14:491–509.
14. Mohanty, S., S. Mishra, P. Jena, B. Jacob, B. Sarkar, and A. Snonawane. 2012. An investigation on the antibacterial, cytotoxic, and antibiofilm efficacy of starch-stabilized silver nanoparticles. Nanomedicine 8:916–924.
15. Aoshima, H., K. Kokubo, S. Shirakawa, M. Ito, S. Yamana, and T. Oshima. 2009. Antimicrobial activity of fullerenes and their hydroxylated derivatives. Biocontrol. Sci. 14:69–72.
16. Prylutska, S., A.P. Burlaka, P.P. Klymenko, I.I. Grynyuk, Y.I. Prylutskyy, C. Schutze, and U. Ritter. 2011. Using water-soluble C60 fullerenes in anticancer therapy. Cancer Nanotechnol. 2:105–110.
17. Shoji, M., E. Takahashi, D. Hatakeyama, Y. Iwai, Y. Morita, R. Shirayama, N. Echigo, H. Kido, S. Nakamura, T. Mashino, T. Okutani, and T. Kuzuhara. 2013. Anti-influenza activity of c60 fullerene derivatives. PLoS One 8: e66337.
18. Montellano, A., T. Da ROS, A. Bianco, and M. Prato. 2011. Fullerene C 60 as a multifunctional system for drug and gene delivery. Nanoscale 3:4035–4041.
19. Rabin, N., Y. Zheng, C. Opoku-Temeng, Y. Du, E. Bonsu, and H. Sintim. 2015. Agents that inhibit bacterial biofilm formation. Future Med. Chem. 7:647–671.
20. Jakobsen, T.H., M.V. Gennip, R.K. Phipps, M.S. Shanmugham, L.D. Christensen, M. Alhede, M.E. Skindersoe, T.B. Rasmussen, K. Friedrich, F. Uthe, P.Q. Jensen, C. Moser, K.F. Nielsen, L. Eberl, T.O. Larsen, D. Tanner, N. Hoiby, T. Bjarnsholt, and M. Givskov. 2012. Ajoene, a sulfur-rich molecule from garlic, inhibits genes controlled by quorum sensing. Antimicrob. Agents Chemother. 56: 2314–2325.
21. Safavi, A., N. Maleki, and M. Doroodmand. 2012. Comparative investigation of chemical vapor deposition of palladium nanoparticles on different carbon substrates. Fuller. Nanotub. Car. N. 20:56–71.
22. Tsumoto, H., S. Kawahara, Y. Fujisawa, T. Suzuki, H. Nakagawa, K. Kohda, and N. Miyata. 2010. Syntheses of water-soluble [60] fullerene derivatives and their enhancing effect on neurite outgrowth in NGF-treated PC12 cells. Bioorg. Med. Chem. Lett. 20:1948–1952.
23. Safavi, A., N. Maleki, M.M. Doroodmand, and M.M. Koleini. 2009. Carbon nanostructures as catalytic support for chemiluminescence of sulfur compounds in a molecular emission cavity analysis system. Anal. Chim. Acta 644:61–67.
24. Percival, S.L., K.E. Hill, D.W. Williams, S.J. Hooper, D.W. Thomas, and J.W. Costerton. 2012. A review of the scientific evidence for biofilms in wounds. Wound Repair Regen. 20:647–657.
25. Darabpour, E., N. Kashef, S.M. Amini, S. Kharrazi, and G. Esmaeeli Djavid. 2017. Fast and effective photodynamic inactivation of 4-day-old biofilm of methicillin-resistant *Staphylococcus aureus* using methylene blue-conjugated gold nanoparticles. J. Drug Deliv. Sci. Technol. 37:134–140.
26. Rosa, L.P., F.C. da Silva, S.A. Nader, G.A. Meira, and M.S. Viana. 2015. Antimicrobial photodynamic inactivation of *Staphylococcus aureus* biofilms in bone specimens using methylene blue, toluidine blue ortho and malachite green: an in vitro study. Arch. Oral Biol. 60:675–680.
27. Sharma, M., L. Visai, F. Bragheri, I. Cristiani, P.K. Gupta, and P. Speziale. 2008. Toluidine blue-mediated photodynamic effects on *staphylococcal* biofilms. Antimicrob. Agents Chemother. 52:299–305.
28. Darabpour, E., N. Kashef, and S. Mashayekhan. 2016. Chitosan nanoparticles enhance the efficiency of methylene blue-mediated antimicrobial photodynamic inactivation of bacterial biofilms: an in vitro study. Photodiagn. Photodyn. Ther. 14:211–217.

29. Wu, X., R.R. Santos, and J. Fink-Gremmels. 2015. Analyzing the antibacterial effects of food ingredients: model experiments with allicin and garlic extracts on biofilm formation and viability of *Staphylococcus epidermidis.* Food Sci. Nutr. 3:158–168.
30. Gopal, R., Y.G. Kim, J.H. Lee, S.K. Lee, J.D. Chae, B.K. Son, C.H. Seo, and Y. Park. 2014. Synergistic effects and antibiofilm properties of chimeric peptides against multidrug-resistant *Acinetobacter baumannii* strains. Antimicrob. Agents Chemother. 58:1622–1629.
31. Gordya, N., A. Yakovlev, A. Kruglikova, D. Tulin, E. Potolitsina, T. Suborova, D. Bordo, C. Rosano, and S. Chemysh. 2017. Natural antimicrobial peptide complexes in the fighting of antibiotic resistant biofilms: *Calliphora vicina* medicinal maggots. PLoS One 12:e0173559.
32. Shrestha, A., Z. Shi, K.G. Neoh, and A. Kishen. 2010. Nanoparticulates for antibiofilm treatment and effect of aging on its antibacterial activity. J. Endod. 36:1030–1035.
33. Kifer, D., V. Mužinić, and M.Š. Klarić. 2016. Antimicrobial potency of single and combined mupirocin and monoterpenes, thymol, menthol and 1, 8-cineole against *Staphylococcus aureus* planktonic and biofilm growth. J. Antibiot. (Tokyo) 69:689–696.
34. Xu, W., X. Zhu, T. Tan, W. Li, and A. Shan. 2014. Design of embedded-hybrid antimicrobial peptides with enhanced cell selectivity and anti-biofilm activity. PLoS One 9: e98935.
35. Walker, N.J. 2002. A technique whose time has come. Science 296:557–559.
36. Li, X., Y.C. Yeh, K. Giri, R. Mout, R.F. Landis, Y.S. Prakash, and V.M. Rotello. 2015. Control of nanoparticle penetration into biofilms through surface design. Chem. Commun. 51:282–285.
37. Vickery, K., H. Hu, A.S. Jacombs, G. Dip, D.A. Bradshaw, and A.K. Deva. 2013. A review of bacterial biofilms and their role in device-associated infection. Healthc. Infect. 18:61–66.
38. Liu, C., J. Guo, X. Yan, Y. Tang, A. Mazumder, S. Wu, and Y. Liang. 2016. Antimicrobial nanomaterials against biofilms: an alternative strategy. Environ. Rev. 25:225–244.
39. Cui, H., C. Ma, and L. Lin. 2016. Co-loaded proteinase K/thyme oil liposomes for inactivation of *Escherichia coli O157: H7* biofilms on cucumber. Food Funct. 7:4030–4040.
40. Saising, J., L. Dube, A.K. Ziebandt, S.P. Voravuthikunchai, M. Nega, and F. Gotz. 2012. Activity of gallidermin on *Staphylococcus aureus* and *Staphylococcus epidermidis* biofilms. Antimicrob. Agents Chemother. 56:5804–5810.
41. Singla, S., K. Harjai, and S. Chhibber. 2013. Susceptibility of different phases of biofilm of *Klebsiella pneumoniae* to three different antibiotics. J. Antibiot. (Tokyo) 66:61.

Address correspondence to:
Abbas Ali Imani Fooladi, PhD
Applied Microbiology Research Center
Systems Biology and Poisonings Institute
Baqiyatallah University of Medical Sciences
Tehran 14359-44711
Iran

E-mail: imanifouladi.a@gmail.com;
imanifouladi.a@bmsu.ac.ir